A System Analysis Approach for Atmospheric Observations and Models: the Mesospheric HO_x Dilemma

Gregory P. Smith,[1] Michael Frenklach,[2] Ryan Feeley,[2] Andrew Packard,[2] and Peter Seiler[2,3]

[1]Molecular Physics Laboratory, SRI International, Menlo Park CA 94025
[2]Dept. of Mechanical Engineering , University of California, Berkeley CA 94720
[3]current address: Honeywell Inc., Minneapolis MN 55419

Abstract. A systematic consistency analysis and optimization procedure is applied to models of representative ozone, OH, and HO_2 observations in the mesosphere and upper stratosphere. The approach considers both measurement and rate parameter uncertainties. The results show some data point inconsistencies and the inability of the accepted photochemical mechanism to predict observations without unfavored large alterations of many rate constants from their consensus values. Optimization results do favor larger rate constants for OH + O, and photolytic ozone and OH production.

11/2/2005
resubmitted to *J. Geophys. Res. Atmospheres*
revised 3/8/2006

1. Introduction.

The study of atmospheric chemistry can be considered a combination of examining the individual reaction, photolysis, and transport steps involved, performing in situ measurements of atmospheric components and properties, and using modeling calculations with these steps to interpret such measurements. This approach validates the model by predicting measurements, and then enables the use of a reliable model to predict various effects. Other systems characterized by such mappings of basic steps onto more complex observations include combustion and various chemical processes. Uncertainties are associated with each aspect of these knowledge systems, both the sets of reaction rate parameters and the observational properties and species to be modeled. Error propagation for a single study considered in isolation often suggests significant model uncertainty, and offers a limited basis for refinement. We will show here how to use new tools of process informatics to analyze quantitatively a representative collection of the available observations along with the basic rate data. The systems approach minimizes model uncertainty (maximizes information) and provides the appropriate forum for comparing disparate measurements.

Mesospheric photochemistry provides an excellent example to illustrate this approach. For unexcited thermal species the chemistry is simple, and only a limited set of atmospheric measurements involving O_3, OH, and HO_2 exist. Yet the observations of the chemically active species of the upper stratosphere and above are poorly predicted by model calculations. The HO_x dilemma[Summers et al., 1997], given much recent notice, offers contradictory trends at 42 and 55 km although the photochemistry is similar. Models of mesospheric observations feature underpredictions of O_3 and HO_2 , while models overpredict OH. Proposals[Summers et al., 1997; Day 2000; Conway et al., 2000] have been advanced to change reaction rate constants for OH + O, O + HO_2 and OH + HO_2 from their recommended most-likely measured values to lessen the discord. While the limited modeling in these papers shows uncomfortably large rate constant changes appear necessary to bring model into agreement with OH measurements, it does not systematically answer the question of whether any more limited combinations of rate constant modifications would suffice, after excluding a few of the measurements if necessary. The new semi-automated analysis method presented here searches out any unexplored solutions. It can prove the lack of acceptable model fits for the data, and also examine the consistency of different measurement datasets.

Our goal therefore is to examine quantitatively and comprehensively the uncertainties of the combined rate parameter - measurements system connected by the modeling, and to locate any acceptable mechanism rate constant values providing acceptable predictive solutions for the HO_x dilemma observations. Any set of rate constant values within certain error bars is allowable, and we wish to find one predicting the largest number of the atmospheric data set within assigned measurement (plus model) uncertainties. This approach is similar to the mechanism optimization procedure we previously used to improve the predictive powers of mechanisms for natural gas combustion.[Smith et al., 1999] Existing field data has also been used to constrain the allowable range of atmospheric rate constant combinations. Examples involve upper tropospheric NO chemistry,[Cohen et al., 2000] and the OH/HO_2 ratio in the lower stratosphere which is mostly controlled by the respective reactions with ozone.[Lanzendorf et al., 2001] New consistency test procedures [Frenklach et al., 2004; Feeley et al., 2004] have been added to the optimization analysis, and will also be used here.

Previous investigators trying to fit their own mesospheric HOx datasets proposed selective rate constant modifications. The MAHRSI data could be predicted[Conway et al., 2000; Summers et al., 1997] by a 50% decrease in $O + HO_2$, or a 20% reduction accompanied by 30% faster $OH + HO_2$. These changes also reduced the model ozone deficit, although all these models were run with ozone constrained to measured values. Sandor and Clancy[1998; Clancy et al., 1994] achieved similar success for their results with a 40-70% reduction in $O + HO_2$. However, Jucks et al. [1998] have data on both OH and HO_2, and found consistency by a 25% reduction in the $(O + HO_2)/(O + OH)$ ratio and a 25% decrease instead in $OH + HO_2$. (Increasing OH + O and OH production is also an option here.) The ozone deficit was not remedied. The two proposed changes did not fit each other's data. Models of the new Aura dataset[Pickett et al., 2006; Canty et al., 2006] done since our efforts were completed suggest 20% increases in the $OH + O$ and $OH + HO_2$ rate constants. The Aura measurements were generally consistent with MAHRSI OH and O_3 at the higher altitudes, and also provide accompanying HO_2 determinations. Again O_3 was fixed in modeling the results, and the ozone deficit issue unsolved, although the HOx dilemma difficulties near 45 km were no longer present in the new data. The data suggest that rate alterations are required. The modifications proposed in the literature were formulated in the context of single datasets, only a few selected reactions are altered. The changes often differ and are sometimes contradictory. Consequently, we need

to examine the entire system of modeled observations and sensitive rate parameters. Also, ozone observations will now be included but not constrained. A measure of observation compatabilities and a suggested group of rate modifications, after considering all the various possibilities and measurements, will result.

2. Method

The process begins with the selection of a representative and modelable set of species measurements above 40 km from the literature (as of 2002), along with a liberal estimate of error bars for each "target experiment" (from noise, calibration, and model parameter water and radiation uncertainties). This search led to 2 sets of MAHRSI measurements of OH by limb UV occultation[Summers et al., 1997; Conway et al., 2000], a small group of high altitude balloon determinations of OH and HO_2 concentrations by far IR emission spectroscopy,[Jucks et al., 1998; Traub et al., 1990; Chance et al., 1996] and a microwave sounding measurement[Sandor and Clancy, 1998] of HO_2. Each HO_x target requires an accompanying ozone target and a local water concentration for model use because it is highly dependent on these values. Where measured values were not given in a reference, proximate HALOE-UARS values[Russell and Remsberg] were substituted. Three OH decay times in photochemical laboratory reactors[Nizkorodov et al., 2000; Robertson and Smith 2001] were also included. The first probes the OH decrease during a radical chain process after a low yield photolysis of an ozone-hydrogen-inert gas mixture. The second follows OH reactions with H_2O_2 and HO_2 after H_2O_2 photolysis. Table 1 and the supplemental materials (Table S-1) show the selection of 39 targets, with references and altitudes, HALOE sources, and the assigned liberal uncertainty limits.

For each measurement, the appropriate altitude-latitude-time solution for concentrations and rate parameters was obtained from the LLNL 2-D diurnally varying global model,[Kinnison and Connell 1999] which uses the NASA evaluated rate parameters.[Sander et al. 2003] Water concentrations from the experimental papers or HALOE observations were substituted for the model values where different, and a box model simulation was run to convergence (1-6 hours) using the Sandia Senkin code.[Lutz et al., 1987] (When no modifications are needed, negligible concentration changes will occur during box model runs.) The second group of columns in Table 1 shows the deviations of the base model predictions (in %) from the measured target values. The many bold type entries show poor predictability beyond our liberal uncertainties.

Table 2 summarizes target predictability by altitude, with black boxes visually displaying failed agreement. The initial preferred rate parameters fail in modeling many of the experimental results. The excessive underprediction of O_3 and HO_2 is evident, with many MAHRSI determinations of OH overpredicted and lower altitude OH underpredicted by the unvaried model that uses the nominal rate parameters.

We then performed the corresponding box model calculations with sensitivity analysis using the Senkin code[Lutz et al., 1987] to determine the small number of active rate parameters (those with large sensitivities) that control the O_3, OH, and HO_2 predictions. (The sensitivity coefficient $S = dX/X / dk/k$ is the fractional change in model concentration divided by that made in a rate constant.) These active model parameters must be allowed to vary over their estimated uncertainty ranges (the allowed mechanism set) to generate all the possible permissible outcomes of modeling of the target experiment. A set of multiple calculations is performed for each target with the active variables spanning their allowed ranges of values. The selection of rate constant value combinations is determined from a fractional factorial design.[Box and Draper 1987] The results are then fit to a second-order polynomial expression (with cross-terms) for faithful reproduction and interpolation of the full model. This response surface now returns any allowable mechanism's model results efficiently by evaluation of polynomial functions. The active variables, which contribute differently to the predictions for the different targets, are shown in Table 3, with their evaluated low temperature uncertainty ranges.[Sander et al., 2003]

The final analysis step involves construction, evaluation, and analysis of an error or objective function. If E_K is the measured value for the target experiment K and $M_K(k_1,k_2,...J_1,...)$ is the model result evaluated at the particular selection of variables, then $\Phi^2 = \Sigma_K \delta_K \omega_K (E_K - M_K(k_1,k_2,...J_1,...))^2$. Here ω is an uncertainty-dependent weighting factor for the target; most often, and in this work, $\omega = \Delta E_K^{-2}$. The delta function δ can be set to 0 if M is within the predesignated error limit ΔE of E, or for a straight optimization $\delta = 1$. Optimization routines, like fmincon from Matlab used here, search for vector solutions minimizing Φ. Penalties for large changes to the k_I variables, or other formulations, can also be added to the objective function.

If we use the delta function formulation, we hope to find a solution consistent with all error bar constraints, $\Phi=0$, which implies a consistent dataset. If this fails, one can increase effective ΔE values until $\Phi = 0$ and an acceptable solution is found possible. This is done by introducing a slack variable t to be minimized, subject to $| E_K - M_K | < \Delta E_K + t$ for all K, and

limited to the allowed rate constant ranges. We determine the smallest value of t added to all the target experiment uncertainties, for which an allowed kinetic model solution predicts all targets within the enlarged error limits. Derivatives of Φ or of t_{MIN} can be taken with respect to the ΔE_K or the bounds on k_I (Lagrange multipliers)[Feeley et al. 2004] to see where the greatest influence to obtaining a consistent solution lies.

The selection of uncertainty limits for the measurements involves some estimation, and alternative choices are possible. For OH and HO_2, our first contributions come from the estimates in the referenced literature, usually one standard deviation values. Because we chose our targets to be representative of the data sets, larger differences than 1-σ were judged improbable. The Jucks values[Jucks et al., 1998] were read from the published graph. We added 5% to one set of HO_2 precision numbers given [Sandor and Clancy, 1998] to account for possible calibration errors. Second, possible modeling errors for the individual measurements must also be accounted for. The main sources are effects from uncertain local water concentrations and local model intensities of the solar flux (with respect to O_3, O_2, and H_2O photolysis rates). We used the sensitivity coefficients to propagate the effects of model variations of 20% in water concentration, 20% in VUV O_2 photolysis light, and 10% in UV O_3 photolysis light to the target predictions. Estimated modeling uncertainty effects are 6-8% for OH, 5-6% for HO_2, and 2-4% for O_3. These values were added in quadrature to the measurement uncertainties to provide the uncertainty bounds used in this study and shown in Table 1. (This also indirectly extends the range beyond the 1-σ measurement bounds.) For ozone, high accuracies are usually claimed for most determinations, and are confirmed by comparisons and variabilities in co-located Haloe data. We have allowed $\pm$10% bounds for these targets, with larger values where indicated by the data - at high altitudes where the absolute concentrations are low.

The permitted ranges (bounds) for the active rate constants in the optimization were chosen from the estimated NASA panel uncertainties at 250K (one standard deviation), which are typically 50% above room temperature values. The low 10% uncertainties given for $O + O_2 + M \rightarrow O_3 + M$ and $O + HO_2$ at 298K were increased to 15% and 20%. We doubled the range for $OH + H_2O_2$ to account for extra uncertainty in the actual H_2O_2 concentration in our photolysis experiments.[Robertson and Smith 2001] Extra range was allowed for the reactions OH + O, HO_2 + O, HO_2 + OH, OH + O_3, and O + O_3, to search slightly larger variations of these sensitive

reactions in the optimization and consistency calculations, by multiplying the uncertainties by 1.25. For $O(^1D)$ quenching, the 298K uncertainty provided the bound.

3. Consistency and Optimization Results

We began our analysis by examining the consistency of the data, i.e., can we find a vector solution {k} that allows each model to predict the corresponding data within the predesignated error limit ΔE. This is accomplished by determining the minimum value of additional error t, added to all dataset experiments, required to find such a vector. (Computationally this is another constrained optimization, with the minimization of t added to the limits already applied to the rate constants and model results.) For the observations in Table 1, the minimum value of t was 17.2%, which is unacceptably high. It should be noted that this significant additional error is not required for each experiment, but that it must be added to at least one in order to find an acceptable vector. This section describes the selection of observations for elimination from the analysis to achieve the desired t_{MIN} of zero.

Eliminating pairwise inconsistencies is a necessary (although not sufficient) first step to determining a consistent set of observations. All pairs of experimental observations (I,J) were analyzed individually to generate t_{IJ} values. These values are the added percent uncertainties to each member experiment of a particular pair that are required to make a pair consistent within the allowed rate parameter values, and are plotted in Fig. 1 as bars when greater than zero. The target numbers for the pairs form the X and Y axes, labeled I and J datasets, and are in the order presented in Table 1 (across and down). Several conclusions can be drawn from the visual display of this simple analysis. A "picket fence" of additional pairwise uncertainty is evident for target 31. This inconsistency of the HO_2 target at 70 km for all pairs reflects the inability of any allowed mechanism to predict its value alone without inflating the error limit. Second, note that the two laboratory OH decay rate results from H_2O_2 photolysis (targets 38,39) require almost 3% additional uncertainty each to become consistent, which suggests one of these targets also should be eliminated. Two other measurements, O_3 and OH at 38 km (targets 2,3) [Chance et al., 1996] show many incompatibilities with other results, so as to merit consideration for removal or reanalysis. This behavior even occurs when considering the O_3 and OH data subsets separately. It should not be surprising, since the photochemistry is the same but the low altitude OH model is low and the higher altitude predictions are excessive. The lower altitude bulge of OH underprediction is the puzzling unexplained feature of the HOx dilemma which has been noted in

the past.[Conway et al., 2000] The consistency test procedure here proves it inconsistent with the other results, given our current modeling understanding.

Next we ran the consistency optimization for the entire dataset, minimizing the value of t added to all target uncertainty limits required to find a mechanism capable of predicting all experiments within the enlarged error bounds. Over 17% more is required, as mentioned above. The Lagrange multiplier for each target, $dt_{MIN}/d\Delta E_K$, describes how the required added error is influenced by each target's individual error value.[Feeley et al. 2004] The value for the 38 km OH target in the initial full dataset run is twice that for any of the next 5, the only other significant ones. That suggests this point be dropped from further consideration first in the effort to achieve dataset consistency. The Lagrange multiplier values (sensitivities) with respect to the rate parameters, dt_{MIN}/dk_I, are shown in Table 3 in the Lagrange column, also for this run. They indicate O_2 and O_3 photolysis, ozone recombination, and the 3 O-OH-HO_2 radical rate constants will be the significant optimization parameters. The low values suggest that modestly larger allowed changes in the rates would not significantly improve the consistency measure t_{MIN}.

When the 38 km OH measurement was removed from consideration, the added uncertainty required for consistency (t) dropped to 13%, and upon removal of the 38 km ozone measurement (suggested by further Lagrange multiplier examination and the pairwise inconsistencies) was reduced to 7%. Removal of the 70 km HO_2 and the lab OH decay values mentioned in the pairwise discussion above reduced t_{MIN} to 3%. (One can also demonstrate that this 3% need not be added to all the target uncertainties for this purpose, by optimizing individual t_I values and minimizing the total in a more sophisticated approach. Only one quarter of the targets require any additional error, $t_I>0$, but 3 would require substantial augmentations of their individual uncertainties by 7%.)

Four more target removals, identified by the parenthesis under the Optimization 1 columns in Table 1, are required to reduce t very close to 0. This renders the remaining set essentially consistent, with two targets showing minor 1% excess deviations that can be considered within the precision of the computations. To summarize, eliminating 8 measurements and their models removes inconsistency from the dataset, with 7 appearing to be inconsistent by substantial amounts.

We took the remaining targets and used the optimization process with the δ objective

function option. We allowed a limited range for the local $J(O_2)$ values due to considerations of optical depth coupled with the cross section uncertainty, as follows. A larger 18% change in the oxygen photolysis cross section is needed to produce a 10% change in the local J values at the model altitudes, due to the accumulated effects of the optical thickness of the atmosphere from the altitudes above a local target. Absorption due to a larger overhead cross section reduces local solar flux and J doesn't increase as much as σ. A fortuitously uniform correction factor is derived from a log-log plot of altitude-dependent local $J(O_2)$ vs. column absorption, which shows a nearly constant slope (-.44). The full range span of 30% for $\sigma(O_2)$ given in parenthesis in Table 3 becomes the 17% shown for $J(O_2)$.

This procedure leads to the Optimization 1 results shown in Tables 1and 3, for the target prediction deviations and rate variable changes, respectively (in %). Deviations shown in bold type exceed the uncertainty limits. Two additional HO_x targets are missed slightly by the optimization, as mentioned above. Table 2 presents those targets with excessive model deviations as black boxes, for starting and optimized mechanisms, arranged by altitude. While an improvement is noted over the original base mechanism model, the results still fail to fit OH observations adequately and consistently, even when omitting consideration of the lowest altitude targets. Note that the missed or excluded targets suffer O_3 overprediction and HO_x underprediction (except 55km OH). This occurs mostly at lower altitudes and is opposite to the unoptimized situation. (The contradiction between lower and high altitude OH results has been noted previously[Conway et al., 2000] and mentioned above.)

Table 3 shows that to provide optimized predictability, a high price has been paid in rate parameter modifications as well. Oxygen photolysis is increased greatly to make more ozone, and 3 O-HO_x reaction rates and the recombination forming ozone are considerably changed. A reduction in $O + HO_2$ and an increase in $OH + HO_2$ was previously used in a model with fixed O_3 to fit the higher altitude MAHRSI data.[Conway et al., 2000]

The optimized model predictions show no average bias, a desirable feature not required in the current objective function or optimization process. Original ozone model predictions with the nominal parameter values averaged -12% low, but the optimization 1 values average +0.4%. For OH above 40 km, the average +9% overprediction was reduced to +1%. For HO_2 below 70 km, the average -21% underprediction becomes a neutral -3%.

We also tried a series of optimization runs with rate constant terms $(k'-k_0)^2/\Delta k^2$ added to

the objective function in gradually increasing amounts relative to the target errors. This attempts to determine whether an equivalent solution exists with lesser rate constant changes, due to a "shallow well" for Φ values on the response surface with respect to the rate parameter values. In this case, once the weighting of rate constant deviations from nominal was increased enough to produce smaller rate constant modifications in the optimization, performance with respect to target prediction deteriorated significantly.

A recent group of 3 measurements determined an increase (18% at room temperature) in quenching by nitrogen[Ravishankara et al., 2002] compared to the long-standing NASA value, [Sander et al., 2003] which is opposite in direction to the optimization, and hence would push the base mechanism predictions further away from the target values. A new study confirms this.[Takahashi et al., 2005] The main sensitivity is really to the rate constant ratio for $O(^1D)$ reaction with water versus quenching by air, as evident from nearly equal and opposite sensitivities to these two reactions for the HO_x measurements (and negligible sensitivity for ozone targets). However, the most recent accompanying measurements[Takahashi et al., 2005; Dunlea and Ravishankara, 2004] for the water reaction rate agree with the previous recommendation. The base model shortfall in predicting most HOx targets (MAHRSI excepted) drives the optimization toward an increase in this ratio, but the newest rate measurements (quenching increase, ratio decrease) indicate otherwise and would further constrain this option.

The recommended rate constant for $OH + O_3$ has changed in the last two NASA evaluations,[Sander et al., 2003] with an increase and then recently a partial retreat. The values used in the base mechanism and LLNL model for this work ($1.5 \times 10^{-12}\ e^{-880/T}$) are from the 2000 evaluation current at the start of our efforts. The latest 2003 values ($1.7 \times 10^{-12}\ e^{-940/T}$) are 6% lower at 298K and 11% lower at 250K, the average target temperature. The optimization favored even lower values, and the uncertainty limits used are sufficiently large to accommodate this shift in central value without requiring refinement of the setup. The -18% optimization change becomes ~-7% relative to the more recent recommendation. One laboratory experimental target, OH decay after photolysis of O_3/H_2,[Nizkorodov et al., 2000] is highly sensitive to this reaction, and a revised base mechanism would predict too slow a decay by 10%. This target would then qualify as an initial miss, remedied in the optimization. Since the analysis in the experimental paper supported the increase in the $OH + O_3$ rate constant, these results are not surprising. The only other base mechanism target predictions that would be affected by this

change are HO_x values near 40 km. A 4% or smaller OH increase and HO_2 decrease would result, insignificant with respect to the margins of failure in the model predictions of the measured concentrations.

We can conclude rigorously from the optimization that either substantial changes are required in the model rate parameters, or that larger uncertainty or error (systematic or underestimated) exists in a large number of the atmospheric data points or their simulations, including upper stratospheric measurements and MAHRSI OH. Even with large rate constant alterations, several experiments cannot be consistently modeled with the rest and had to be excluded from further consideration solely by mathematical criteria. No previously unlocated solution for the HOx dilemma can be found. The particular datasets whose analysis, uncertainty, and modeling merit further scrutiny have been identified in the optimization and exclusion process.

4. Multiple Solutions

A second optimized solution was located while using the Matlab routine to search for objective function minima. This solution required generally less drastic rate constant changes, it decreases rather than increases the rate constant for OH + HO_2, and it uses a lower O_3 photolysis rate. Three more targets must be excluded to obtain this solution, but several parameters show little change. In fact, 40% of the active rate parameters could be frozen at their initial central values without causing further deterioration of the optimization fit to the target values, or to the set of consistent targets. Substantial increases are still required for the OH + O rate constant, and the $O(^1D)$ reaction versus quenching ratio (especially when considering the newer measurements). Results are given in Tables 1-3, listed as Optimization 2. Agreement is somewhat worse with respect to the full dataset, especially for OH. Average OH concentrations are overpredicted by 5-10%, although no bias occurs when examining just the retained targets. If one were to restrict the rate parameter uncertainties or changes to smaller individual or cumulative values (probably a more realistic expectation), this result would form the preferred optimized solution and consistent dataset. The decreased rate constant for OH + HO_2 mirrors Jucks' proposed adjustment,[1998] and gives a better fit to his data at the expense of the MAHRSI targets. The pairwise consistency tests (Fig. 1) however do not flag any results from comparing these two data sets, Jucks (targets 4-12) and MAHRSI (targets 13-26).

In light of the above alternate result, the potential for several different viable optimized solutions needs further systematic investigation. These might exist with perhaps differing rate parameter changes or excluded inconsistent targets, or could just be a result of shallow regions on the response surface. Having new information available from the pairwise inconsistencies, and the Lagrange multipliers for the targets in the consistency (t) tests (as sensitivities to the bounds), in addition to the usual examination of the worst target misses in optimization calculations, provides guidance in searching for consistent optimized solutions. The polynomial representation of the response surface also enables a relatively efficient random search for solutions (rate parameter combinations) that are consistent with at least some fixed number of targets. This Monte Carlo approach can be used to find new patterns or starting setups for alternate optimizations. Our first such search efforts found 39 solutions that missed 9-10 atmospheric targets. A qualitatively different optimum solution was not located. The results do show that it is possible to use somewhat different rate constant combinations to achieve similar model improvements, such as adjusting $O(^1D) + H_2O$ or $OH + O_3$ instead of $OH + O$ or $HO_2 + O$. These alternate solutions also suggest some choice among the subset of moderately ill-predicted targets as to which will be outside their limits and thus judged inconsistent. Table S-2 of the supplemental material provides a statistical summary of all satisfactory runs runs.

We can examine this set of modestly acceptable alternate solutions for trends that may suggest some constraints on rate constant values consistent with the selected remaining data. There is a formal procedure available for the type of optimization employed here that can furnish minima and maxima for each rate constant value, beyond which no solution exists that succeeds in predicting the targets within their limits.[Frenklach et al., 2004]. Because many targets are out or near their uncertainty bounds on any trials here, we have not performed this procedure on a necessarily much smaller and more consistent subset. We did examine the Monte Carlo solutions summarized in Table S-2 to see which rate constant adjustments were correlated with each other, and to describe the ranges of rate constants seen in the solution set (Table S-2B). Among the pairs of 10 rate parameter optimization variables, there are 4 showing significant (0.5) correlations from the solutions. Ozone photolysis changes correlate with $O + O_2$ recombination, the $OH + HO_2$ reaction that neutralizes ozone-destroying HOx, and with O_2 photolysis. This would suggest a family of mechanisms where any increase in ozone photolysis can be offset by increasing its formation rate or by reducing the amount of destructive OH. For

similar reasons (and applying to higher altitude targets), a large correlation between water photolysis and the compensating OH + HO_2 rate constant was found among the solutions.

Given the many potential compensatory adjustments involving OH + HO_2, it is not surprising that its variability in the solutions is large, according to Table S-2B. The lowest variability and presumably the strongest preference for alteration belongs to OH + O and HO_2 + O. The most consistent directional bias occurred for the reactions OH + O (faster), O + HO_2 (slower), and oxygen (faster) and ozone photolysis (slower). While there is a preference to decrease the OH + HO_2 rate constant, many solutions in the opposite direction also exist.

A comparison of the Optimization 2 rate constant changes can be made to the previous proposals. We see obvious changes to oxygen and ozone photolysis and recombination to remedy the ozone deficit. The remainder show the greatest similarity to the Jucks'[1998] modifications with changes to OH + O, O + HO_2, OH + HO_2, and $O(^1D)$ + H_2O in the indicated directions. Note however that the Optimization 1 result favors an increase for OH + HO_2 in accord with the MAHRSI[Conway et al., 2000] and Aura[Canty et al., 2006] preferences, so the current effort does not resolve this matter. What is notable in our optimizations is the sizable 30% recommended increase in OH + O, as opposed to the large decrease in O + HO_2 which was used to fit the MAHRSI data.[Conway et al., 2000] This increase for OH + O (plus an increase in OH + HO_2) was also recommended to explain the new Aura HOx data,[Canty et al., 2006] and thus our optimization on the old data supports this result. Some new laboratory measurements also suggest a larger rate constant for OH + O at low temperatures.[Robertson and Smith, 2006]

5. Model Errors

Using this analysis with an easily-run 0-D box model neglects the effects on the local $J(O_3)$ values of the changes in the overhead ozone column as all the rate parameters are varied. The local $J(O_3)$ values are currently assumed to scale at all altitudes. Due to optical thickness this gives faulty results for targets below 50 km. Less variation in J at low altitude is the correct picture. Corrections can be made to the model ozone and HO_x low altitude target calculations after the optimization, but they do not improve these poor results. For optimization 2, the increase in column ozone (to match the ozone targets) is counterbalanced by a lower optimization J value, the column absorption changes <2%, and the corrections to target predictions from non-local effects are negligible(0.5%). Optimization 1 shows increases of 25%

in column absorption at high altitudes, and large corrections (17%) result for targets below 45 km. However, most of these targets were missed or excluded by the optimization, and the corrections did not improve the situation, in general making disagreement worse. The corrections to target model values calculated for Optimization 1 were computed by adjusting each local $J(O_3)$ for the increased column absorption above, by using results from the LLNL model. Results are given in the supplemental material, Table S-3. These effects need to be incorporated into future optimization designs.

A full analysis of the atmospheric HO_x system should also incorporate data from other regions, such as modeling difficulties with the OH/HO_2 ratio in the lower stratosphere.[Lanzendorf et al., 2001] Chlorine and nitrogen oxide chemistries are additional factors to consider for stratospheric data. New laboratory or reactor targets can also be incorporated.

In principle model parameter uncertainties can also be introduced as optimization parameters - here local water concentrations and the use of localized O_2 and O_3 photolysis rates from the LLNL 2-D outputs are the prominent examples. In practice these model parameter uncertainties may also be subsumed as errors propagating into the target uncertainties. The sensitivity coefficients can be used for this error propagation. The treatment above assumed minor model errors in assessing the target uncertainties. As a more drastic model reliability test, an optimization was conducted with ozone target uncertainties increased to 17%, and an extra 10% added to the HO_x targets. The same target inconsistencies and optimization rate parameter changes resulted, although their required magnitudes were halved. This result is given in the supplemental material, Table S-4. Adopting a moderately larger estimate of measurement error does not alter the conclusions.

6. Conclusions

This approach should be adaptable to other realms of the atmosphere, including stratospheric ozone issues, global atmospheric models, the troposphere and pollution issues, plumes, and source term concerns, as well as combustion and other chemical processes, and even astrophysical material observations. The systemic uncertainty analysis can produce an optimized mechanism (or set of allowed, feasible mechanisms) that adequately accounts for the most observations and thus yields the most reliable predictability, and can compute the compatibility

of diverse observations. We envision that this framework will also provide a way to estimate prediction probabilities, evaluate and guide the worth of proposed rate and field measurements, and furnish a convenient tool to place new work and ideas into the context of the previous knowledge of the system. Recent microwave limb sounder measurements of HO_x from balloons and the Aura satellite[Pickett et al., 2005, Canty et al., 2006] already suggest an update. This is a tool that should be used with new observations and kinetics revisions.

The mesospheric O_3 and OH targets in the optimization, largely from MAHRSI, are generally consistent with the new Aura and balloon results.[Pickett et al., 2006] Compared to baseline models, both datasets show higher ozone and lower OH by 15-20%. Of particular note, our optimization effort on the varied set of old data strongly confirms the Aura team's proposal to increase the OH + O rate constant,[Canty et al., 2006] one of the options the older efforts did not promote. It would of course be interesting in the future to add Aura HO_2 and lower attitude results as targets, and see what effect this would have on consistency results and the direction of changes for OH + HO_2.

The quantitative results on modeling the previous HO_x measurements in the upper atmosphere illustrate the inability of the accepted photochemical mechanism to consistently predict observations within liberal error limits without forcing large changes on many rate parameters. The technique provides proof (beyond sound intuition and the limited previous modeling) of the absence of a consistent data/parameter set, and also establishes its existence and identity once certain more contingent conditions and omissions are adopted. A second optimization with more reasonable and stringent constraints on rate alterations fails to account well for the OH data. Results for the lower altitudes are generally inconsistent and even more poorly fit. It is however possible to account for the bulk of higher altitude results via some rate parameter changes - most significantly increasing ozone and the OH + O and $O(^1D) + H_2O$ rate constants. Additional measurements and mechanistic modeling efforts are needed to address the data modeling difficulties, and can readily be incorporated into this analysis framework.

Acknowledgements: Research at SRI was supported by the NASA ITM Physics Program (grant NAG5-11927) and the NSF Aeronomy Program (grant ATM-0233523).. Work at UCB was supported by NSF (grant CTS-0113985). Thanks to Dr. Peter Connell of LLNL for providing his model results, and Dr. David Golden for helpful discussions.

References

Box, G. E. P., and N. R. Draper, "Empirical Model Building and Response Surfaces," Wiley, N.Y., 1987.

Canty, T., H. M. Pickett, R. J. Salawitch, K. W. Jucks, W. A. Traub, and J. W. Waters, "Stratospheric and mesospheric HOx: Initial results from Aura MLS," Geophys. Res. Lett., submitted, 2006.

Chance, K., W. A. Traub, D. G. Johnson, K. W. Jucks, P. Ciarpallini, R. A. Stachnik, R. J. Salawitch, and H. A. Michelsen, "Simultaneous measurements of stratospheric HOx, NOx, and ClOx: comparison with a photochemical model," J. Geophys. Res., 101, 9031-9043, 1996.

Cohen, R. C., K. K. Perkins, L. C. Koch, R. M. Stimpfle, P. O. Wennberg, T. F. Hanisco, E. J. Lanzendorf, G. P. Bonne, P. B. Voss, R. J. Salawitch, L. A. Del Negro, J. C. Wilson, C. T. McElroy, and T. P. Bui, "Quantitative constraints in the atmospheric chemistry of nitrogen oxides: an analysis along chemical coordinates," J. Geophys. Res., 105, 24283, 2000.

Conway, R. R., M. E. Summers, M. H. Stevens, J. G. Cardon, P. Preusse, and D. Offermann, "Satellite observations of upper stratospheric and mesospheric OH: the HOx dilemma," Geophys. Res. Lett., 27, 2613-2616, 2000.

Day, C., "New measurements of hydroxyl in the middle atmosphere confound chemical models," Physics Today, Nov. 2000, p. 17-19.

Dunlea, E. J., and A. R. Ravishankara, "Kinetic studies of the reactions of $O(^1D)$ with several atmospheric molecules," Phys. Chem. Chem. Phys., 6, 2152-2161, 2004.

Feeley, R., P. Seiler, A. Packard, and M. Frenklach, "Consistency of a reaction dataset," J. Phys. Chem. A 108, 9573-9583 , 2004.

Frenklach, M., A. Packard, P. Seiler, and R. Feeley, "Collaborative data processing in developing predictive models of complex reaction systems," Int. J. Chem. Kinet., 36, 57-66, 2004.

Jucks, K. W., D. G. Johnson, K. V. Chance, W. A. Traub, J. J. Margitan, G. B. Ostermann, R. J. Salawitch, and Y. Sasano, "Observations of OH, HO_2, H_2O, and O_3 in the upper stratosphere: implications for HOx photochemistry," Geophys. Res. Lett., 25, 3935-3938, 1998.

Kinnison, D. E., and P. S. Connell, "1.2.6 LLNL 2-D Model," in *Models and Measurements Intercomparison II*, J. H. Park, M. K. W. Ko, C. H. Jackman, R. A. Plumb, J. A. Kaye, and K. H. Sage, ed., NASA/TM-1999-209554, p. 54-57, 1999.

Lanzendorf, E. J., T. F. Hanisco, P. O. Wennberg, R. C. Cohen, R. M. Stompfle, and J. G. Anderson, "Comparing atmospheric HO_2/OH to modeled HO_2/OH: Identifying discrepancies with reaction rates," Geophys. Res. Lett., 20, 967-970, 2001.

Lutz, A. E., R. J. Kee, and J. A. Miller, " SENKIN: A Fortran Program for Predicting Homogeneous Gas Phase Chemical Kinetics with Sensitivity Analysis," Sandia National Laboratories, Report SAND87-8248, 1987.

Nizkorodov, S. A., W. W. Harper, B. W. Blackmon, and D. J. Nesbitt, "Temperature dependent kinetics of the OH/HO_2/O_3 chain reaction by time-resolved IR laser absorption spectroscopy," J. Phys Chem A 104, 3964-3973 , 2000.

Pickett, H. M., B. J. Drouin, T. Canty, L. J. Kovalenko, R. J. Salawitch, N. J. Livesey, W. G. Read, J. W. Waters, K. W. Jucks, and W. A. Traub, "Validation of Aura MLS HO_x measurements with remote-sensing balloon instruments," Geophys. Res. Lett., 33, L01808, 2005..

Ravishankara, A. R., E. J. Dunlea, M. A. Blitz, T. J. Dillon, D. E. Heard, M. J. Pilling, R. S. Strekowshi, J. M. Nicovich, and P. H. Wine, "Redetermination of the rate coefficient for the reaction of $O(^1D)$ with N_2," Geophys. Res. Lett., 29, 1745, 2002.

Robertson, R., and G. P. Smith, " Temperature Dependence of O + OH at 136-377 K using Ozone Photolysis," J. Phys. Chem. A, in press (2006).

Robertson, R., and G. P. Smith, unpublished data, 2001.

Russell III, J. M., and E. E. Remsberg, HALOE Web site, http://haloedata.larc.nasa.gov

Sander, S. P., R. R. Friedl, D. M. Golden, M. J. Kurylo, R. E. Huie, V. L. Orkin, G. K. Moortgat, A. R. Ravishankara, C. E. Kolb, M. J. Molina, and B. J. Finlayson-Pitts, *Chemical Kinetics and Photochemical Data for Use in Stratospheric Modeling - Evaluation 14*, JPL Publication 02-25; Jet Propulsion Laboratory, California Institute of Technology: Pasadena, CA, 2003, jpldataeval.jpl.nasa.gov.

Sandor, B. J., and R. T. Clancy, "Mesospheric HOx chemistry from diurnal microwave observations of HO_2, O_3, and H_2O," J. Geophys. Res., 103, 13337-13351, 1998.

Smith, G. P., D. M. Golden, M. Frenklach, M., N. W. Moriarty, B. Eiteneer, M. Goldenberg, C. T. Bowman, R. K. Hanson, S. Song, W. C. Gardiner, V. Lissianski, and Z. Qin, GRI-Mech 3.0 Web site, http://www.me.berkeley.edu/gri_mech/, 1999.

Summers, M. E., R. R. Conway, D. E. Siskind, M. H. Stevens, D. Offermann, M. Riuese, P. Preusse, D. F. Strobel, and J. M. Russell III, "Implications of satellite OH observations for middle atmospheric H_2O and ozone," Science, 277, 1967-1970 , 1997.

Takahashi, K., Y. Takeuchi, and Y. Matsumi, "Rate constants of the $O(^1D)$ reactions with N_2, O_2, N_2O, and H_2O at 295 K," Chem. Phys. Lett., 410, 196-200, 2005.

Traub, W. A., D. G. Johnson, and K. V. Chance, "Stratospheric hydroperoxyl measurements," Science, 247, 446-449, 1990.

Table 1. Target Experiments and Optimization Results;
Percentage uncertainty limits and model deviations from measurements given
Shaded **bold** values exceed uncertainty limits; ( ) indicates exclusion from the optimization

Ref.	Alt.	error	limit	%	initial	miss	%	Opt. 1			Opt. 2		
	(km)	O3	OH	HO2	O3	OH	HO2	O3	OH	HO2	O3	OH	HO2
(1)	38	9	13	22	**+19**	**−50**	**−29**	(**+38**)	(**−46**)	−19	(**+42**)	(**−50**)	−6
(2)	40	10	12	14	+1	**−20**	−3	(**+16**)	**−13**	+14	(**+19**)	(**−20**)	(**+32**)
(2)	45	10	11	14	**−16**	−10	**−20**	+5	−11	+11	+3	−10	+13
(2)	50	10	10	14	**−22**	−9	**−26**	−5	(**−13**)	+2	−5	−10	+4
(3)*	43	10	19		**−24**	**−22**		−10	(**−24**)		−7	**−23**	
(3)*	50	10	17		**−26**	**+18**		−10	+13		−10	+17	
(3)*	55	10	19		**−18**	**+30**		−4	+19		−1	(**+27**)	
(3)*	65	10	20		**−20**	+12		−6	+1		+1	+4	
(3)*	73	25	22		−11	−11		+7	−22		+14	−20	
(4)*	50	10	25		−8	**+33**		+6	+23		+10	**+30**	
(4)*	55	10	25		**−14**	**+42**		+1	(**+30**)		+3	(**+38**)	
(5)	55	10		20	**−12**		**−26**	+2		−2	+5		+2
(5)	61	15		15	**−24**		**−37**	−12		**−16**	−7		−15
(5)	70	30		15	−1		**−56**	+19		(**−44**)	+28		(**−44**)
(6)*	49	10		10	−9		**−32**	+10		−7	+9		−6
(6)*	40	10		10	**−11**		**−19**	+4		−10	+6		+10
(7)+	O3,H2		5			+2			+5			-4	
(8)+	H2O2		2			**−11**			−0.2			-1.4	
(8)+	H2O2		2			**−32**			(**−25**)			(**−24**)	

* HALOE O_3
+ Initial OH also an optimization variable; targets are decay times
(1) Chance et al., 1996; Far InfraRed Spectrum (balloon overhead thermal emission).
(2) Jucks et al., 1998; Far InfraRed Spectrum (balloon overhead thermal emission); high altitude results dependent on altitude distribution assumptions.
(3) Conway et al., 2000; MAHRSI solar excited UV emission (limb).
(4) Summers et al., 1997; MAHRSI solar excited UV emission (limb).
(5) Sandor and Clancy, 1998; microwave enission (telescope).
(6) Traub et al., 1990; Far InfraRed Spectrum (balloon overhead thermal emission).
(7) Nizkorodov et al., 2000; lab decay of OH after partial O_3 photolysis (OH, H, O_3).
(8) Robertson and Smith, 2001; lab decay of OH in H_2O_2 after photolysis.

Table 2. Atmospheric Target Prediction Failures, Model - Measurement > Uncertainty. Sorted by altitude, with failures shown by black squares, success by **, and lack of a target by a dash or blank. See Table 1 footnotes for full references.

Ref.	1st Author	Alt.	initial model			Opt. 1			Opt. 2		
		(km)	O3	OH	HO2	O3	OH	HO2	O3	OH	HO2
1	Chance 96	38	■	■	■	■	■		■	■	
2	Jucks 98	40	**	■		■	■		■	■	■
6	Traub 90	40	■	---	■	**	---			---	
3	Conway 00	43	■	■	---		■	---		■	---
2	Jucks 98	45	■		■						
6	Traub 90	49		---	■		---			---	
2	Jucks 98	50	■		■		■				
3	Conway 00	50	■	■							
4	Summers 97	50		■						■	
3	Conway 00	55	■	■						■	
4	Summers 97	55	■	■			■			■	
5	Sandor 98	55	■		■						
5	Sandor 98	61	■		■			■			
3	Conway 00	65	■		---			---			---
5	Sandor 98	70		---	■		---	■		---	■
3	Conway 00	73									

Table 3. Optimization Variables. Deviations from central recommended values, and Lagrange Multipliers for consistency parameter

Reaction	Range	Lagrange	Opt. 1	Opt. 2
$O+O2 \rightarrow O3$	±20%	+.011	+13.2%	+9.8%
$O+O3 \rightarrow 2O2$	±50%	−.003	−32.8%	0%
$O(^1D)+air \rightarrow O$	±20%	−.001	−15.4%	0%
$O(^1D)+H2O \rightarrow 2OH$	±30%	+.002	+19.5%	+20.2%
$H+O2/O3 \rightarrow HO2/OH$	±60%	+.004	+59.3%	0%
$OH+O3 \rightarrow HO2+O2$	±35%	−.001	−18.1%	0%
$OH+O \rightarrow H+O2$	±35%	+.006	+32.1%	+27.8%
$HO2+O \rightarrow OH+O2$	±30%	−.017	−6.8%	−12.8%
$HO2+OH \rightarrow H2O+O2$	±50%	−.006	+23.4%	−11.0%
$OH+H2O2 \rightarrow HO2+H2O$	±35%	−.011	−15.8%	−11.6%
$O2+hv \rightarrow 2O$	±17(30)%	+.019	+17.0%	+16.3%
$O3+hv \rightarrow O2+OorO(^1D)$	±30%	−.014	-3.5%	−13.6%
$H2O+hv \rightarrow H+OH$	±35%	−.001	+34.9%	0%

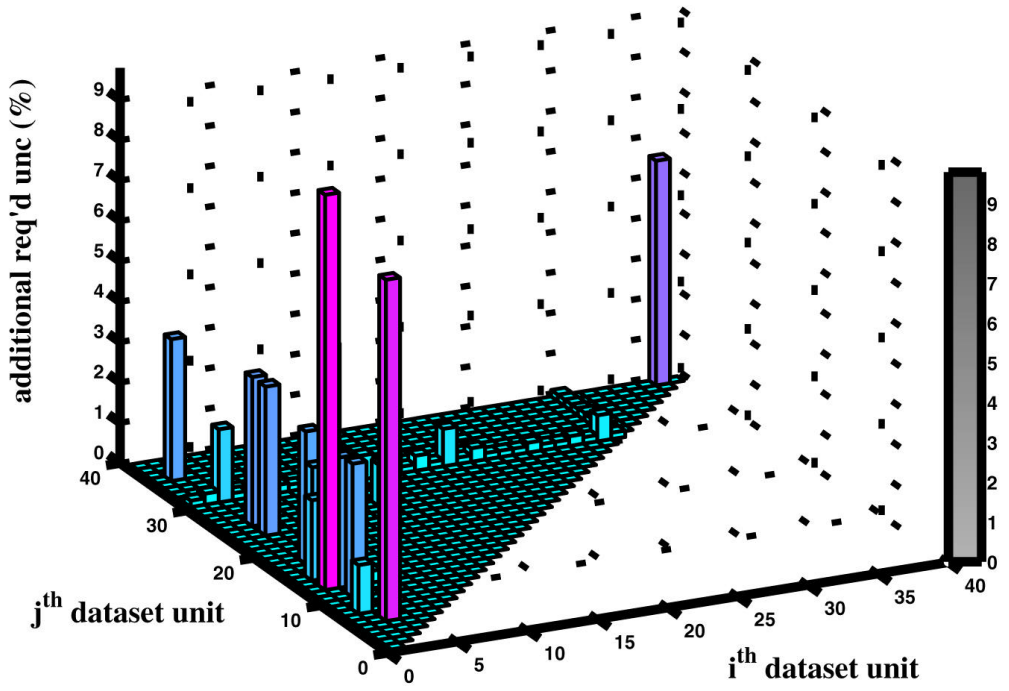

Figure 1. Inconsistency plots for observational target pairs. Value of t on the Z-axis is the added error needed to make a pair self-consistent within model and measurement uncertainties, and hence fit with a feasible mechanism. (Coloration for visual contrast only.)

Supplemental material:

Table S-1. Target details and values. (* HALOE Ozone)

Ref.	Alt.	location	O_3	OH	HO_2	H_2O	$J(O_2)$	$J(O_3)$
	km		ppm	ppb	ppb	ppm	10^{-10}/s	/s
(1)	38	37N Sept. 11am	7.15	.187	.18	5.24	1.55	.00118
(2)	40	70N Apr. 9am	6.4	.134	.143	6.60	1.78	.00128
(2)	45	FIRS-2	4.5	.39	.26	6.84	3.76	.00314
(2)	50		2.6	.70	.42	6.95	6.18	.00625
(3)	43	50N Aug. 12n	6.17*	.374		6.12*	3.99	.00308
(3)	50	MAHRSI	2.94*	.547		6.41*	6.78	.00669
(3)	55		1.8*9	.635		6.28*	8.36	.00790
(3)	65		0.63*	1.61		6.32*	15.3	.00840
(3)	73		0.21*	4.2		6.04*	25.9	.00833
(4)	50	32N Nov. 11am	2.69*	.508		5.86	6.60	.00651
(4)	55	MAHRSI	1.81*	.594		5.99	8.14	.00808
(5)	55	32N Nov. 11am	1.75		.54	6.30	8.14	.00808
(5)	61		1.1		.85	6.51	10.7	.00862
(5)	70		0.24		2.86	6.51	19.8	.00885
(6)	49	32N May 3pm	2.7*		.447	6.04*	6.71	.00676
(6)	40		6.73*		.194	5.40*	3.31	.00234
(7)	O3,H2	9.1t H2 .78t O3 .05% dssn.		806μs	243K 12t CO_2 11ppmO*+4ppmO			
(8)	H2O2	0.48t H2O2 4.5% dssn.		27.9μs	7t H_2O, 33.6t N_2			
(8)	H2O2	0.48t H2O2 1.5% dssn.		35.8μs				

(1) Chance et al., 1996 (2)Jucks et al., 1998. (3)Conway et al., 2000. (4) Summers et al., 1967. (5) Sandor and Clancy, 1998. (6) Traub et al., 1990. (7) Nizkorodov et al., 2000. (8) Robertson and Smith, 2001.

* HALOE sources: (3): Monthly means at sunset Aug. 1997 48&52N; 65&73km 8/31/97 50N
(4): Monthly means at sunset Nov. 1994 36N
(6):Monthly means at sunset May 1992 32N

Table S-2. Target and parameter statistics for random solutions successfully accounting for 28 or more target values.

A. Fraction of successful runs consistent with target.

Ref.	Alt.(km)	O3	OH	HO2
(1)	38	0	0	0.91
(2)	40	0.06	0.15	0.62
(2)	45	1.00	0.19	0.95
(2)	50	0.97	0.18	1.00
(3)	43	0.51	0.15	
(3)	50	0.42	0.82	
(3)	55	1.00	0.81	
(3)	65	0.96	0.94	
(3)	73	1.00	0.67	
(4)	50	0.72	0.81	
(4)	55	1.00	0.67	
(5)	55	0.97		1.00
(5)	61	1.00		0.85
(5)	70	0.97		0
(6)	49	0.93		0.76
(6)	40	0.97		0.96

B. Fraction of the allowable rate parameter ranges seen in the above sampled random solutions.

Reaction	Range
O+O2	74%
$O(^1D)$+H2O	86%
H+O2/O3	62%
OH+O3	89%
OH+O	25%
HO2+O	36%
OH+HO2	73%
O2+hv	37%
O3+kv	46%
H2O+hv	86%

Table S-4B. Rate constant changes for S-4A optimization.

Reaction	Change
O+O2	+6.6%
$O(^1D)$+H2O	+16.5%
H+O2/O3	+32.3%
OH+O3	-10.8%
OH+O	+26.1%
HO2+O	-8.6%
OH+HO2	-0.2%
O2+hv	+17.0%
O3+kv	+2.2%
H2O+hv	+16.7%

Table S-3. Corrections to Optimization 1 model values due to ozone optical depth (%). **Bold** indicates that the newly-added deviation extends beyond the target uncertainty. *Italics* indicate improved agreement.

Ref.	Alt.(km)	O3	OH	HO2
(1)	38	+13.	-18.3	**-4.1**
(2)	40	+16.6	-24.8	*−6.*
(2)	45	**+10.4**	**-4.9**	-3.3
(2)	50	+3.6	-0.5	-1.
(3)	43	*+13.*	-9.6	
(3)	50	+2.1	-0.3	
(3)	55	+1.6	0	
(3)	65	0		
(3)	73	0		
(4)	50	+2.6	-0.3	
(4)	55	+1.9	0	
(5)	55	+2.3		0
(5)	61	0		
(5)	70	0		
(6)	49	**+6.6**		-2.
(6)	40	**+22.6**		**-6.3**

Table S-4A. Optimization results with large model uncertainties incorporated (% miss). O_3 uncertainties at 17%, 10% added to HO_x target uncertainties. A **bold** value exceeds the higher uncertainty limit.

Ref.	Alt.(km)	O3	OH	HO2
(1)	38	**32**	**-46**	-17
(2)	40	12	-13	16
(2)	45	-3	-9	8
(2)	50	-12	-12	-0
(3)	43	-15	-22	
(3)	50	-17	14	
(3)	55	-12	-22	
(3)	65	-15	3	
(3)	73	-5	-19	
(4)	50	-1	26	
(4)	55	-7	33	
(5)	55	-6		-4
(5)	61	**-19**		-18
(5)	70	7		**-44**
(6)	49	2		-9
(6)	40	-2		-3

References: (1) Chance et al., 1996 (2)Jucks et al., 1998. (3)Conway et al., 2000. (4) Summers et al., 1967. (5) Sandor and Clancy, 1998. (6) Traub et al., 1990.